Journal of Electronic Materials
https://doi.org/10.1007/s11664-021-09425-2

ORIGINAL RESEARCH ARTICLE

Plasma-Assisted Epitaxy of Piezoelectric $Sc_xAl_{1-x}N$ Films on Sapphire for Use in Harsh-Environment Microwave Acoustic Sensors

Morton Greenslit[1,3] · Mauricio Pereira da Cunha[2,3] · Robert J. Lad[1,3]

Received: 23 August 2021 / Accepted: 29 December 2021

Abstract

The $Sc_xAl_{1-x}N$ wurtzite structure has been shown theoretically and experimentally to exhibit significantly higher piezoelectric coupling compared to pure AlN. In this work, a plasma-assisted epitaxial growth method has been used to synthesize epitaxial (0002) $Sc_xAl_{1-x}N$ films on c-sapphire substrates from $x = 0.07$ to 0.30 by co-evaporating high-purity Sc and Al sources in the presence of a nitrogen plasma generated by an RF plasma source. Epitaxial $Sc_xAl_{1-x}N$ films with highly oriented (0002) grains and in-plane registry were produced on c-sapphire substrates that were pre-exposed to the nitrogen plasma to form an oxynitride seed layer. Growth of $Sc_xAl_{1-x}N$ films was carried out at 930°C under both metal-rich and N-rich conditions using precisely controlled Sc, Al, and N-plasma fluxes. Metal-rich depositions yielded non-(0002)-oriented $Sc_xAl_{1-x}N$ grains and intermetallic ScAl grains. Nitrogen-rich growth with a Sc/Al flux ratio of 1/3 produced the best (0002) epitaxy as determined by x-ray diffraction analysis. Surface acoustic wave resonator (SAWR) devices were fabricated from 500-nm-thick $Sc_xAl_{1-x}N$ and AlN films to extract their electromechanical coupling coefficients, k^2. As the Sc concentration in the films increases, the degree of (0002) epitaxy is reduced, yet the value of k^2 increases because there is more Sc in the wurzite lattice despite the decreased level of (0002) grain alignment. The use of a 10-nm-thick Si_xN_y capping layer on top of the $Sc_xAl_{1-x}N$ films aids in preventing etching during SAWR device photolithography and also helps hinder film oxidation up to 800°C.

Keywords Scandium aluminum nitride · aluminum oxynitride · plasma-assisted epitaxy · piezoelectric film · surface acoustic wave resonator

Introduction

Typical piezoelectric materials such as lead zirconate titanate (PZT) or barium titanate (BTO) have large piezoelectric coupling coefficients, d_{33}, near room temperature but lose their piezoelectricity above –300°C. The AlN wurtzite structure retains piezoelectricity to at least 1000°C, and AlN films can be grown using a wide range of techniques, making AlN an attractive high-temperature piezoelectric material for harsh-environment, high-temperature sensor applications.[1–5] The addition of scandium into the AlN wurtzite lattice to form a $Sc_xAl_{1-x}N$ alloy has been both theoretically[6] and experimentally[7] shown to increase the d_{33} value by up to 500% compared to pure AlN.

By far the most common method that has been used to synthesize $Sc_xAl_{1-x}N$ films to date is RF magnetron sputtering,[7–17] which allows for rapid reproducible film growth with a fixed uniform composition, but a disadvantage of this approach is the need to install a new sputtering target to change the $Sc_xAl_{1-x}N$ film stoichiometry. In addition, the high deposition rates and low deposition temperatures typically employed during sputtering lead to a multitude of defects and poorer crystal quality than can be achieved using high-temperature growth methods such as molecular beam epitaxy (MBE),[18–22] halide vapor transport epitaxy (HVTE),[23,24] or metal organic chemical vapor deposition (MOCVD).[25,26] The nitrogen plasma-assisted MBE approach used in this work allows accurate control of Sc, Al, and N fluxes at a growth temperature of 930°C in an ultra-high vacuum (UHV) environment which yields a range of well-defined epitaxial $Sc_xAl_{1-x}N$ alloy film compositions.

✉ Morton Greenslit
morton.greenslit@maine.edu

[1] Department of Physics & Astronomy, University of Maine, Orono, ME 04469-5708, USA

[2] Department of Electrical & Computer Engineering, University of Maine, Orono, ME 04469-5708, USA

[3] Frontier Institute for Research in Sensor Technologies (FIRST), University of Maine, Orono, ME 04469-5708, USA

Reported investigations of $Sc_xAl_{1-x}N$ films grown by sputtering and other growth methods have primarily focused on applications of $Sc_xAl_{1-x}N$ films for LEDs,[18] electron transport,[19–22,27] and surface acoustic wave resonator (SAWR) devices.[7–18] To characterize SAWR device response, several resonator designs have been proposed[7–18] and the emphasis has been on optimizing $Sc_xAl_{1-x}N$ film thickness rather than exploring the influence of the Sc concentration. In this paper, we report structural and compositional results for $Sc_xAl_{1-x}N$ films grown over a wide range of Sc/Al ratios on c-sapphire substrates. Furthermore, $Sc_xAl_{1-x}N$-based SAWR devices have been fabricated, and the electromechanical coupling coefficients, k^2, have been measured from SAWR devices operating near 455 MHz. The measured k^2 values can be directly correlated with the piezoelectric coupling coefficients, d_{33}, and the results indicate that the piezoelectric response is highly dependent on the epitaxial quality as well as the Sc content in the $Sc_xAl_{1-x}N$ films.

For application of $Sc_xAl_{1-x}N$ films and SAWR devices in wireless sensor systems for high-temperature, harsh environments such as those encountered in the power generation industry,[28,29] the films and associated sensor device must be stable under oxidizing conditions at temperatures as high as 1000°C. A more negative Gibbs free energy of formation for Sc_2O_3 compared to Al_2O_3[27] causes $Sc_xAl_{1-x}N$ to oxidize at lower temperatures and more rapidly than AlN films.[20] Thus, film oxidation may be a limiting factor for the application of $Sc_xAl_{1-x}N$-based piezoelectric films. We show data that illustrates that a 10-nm-thick Si_xN_y capping layer is effective at hindering oxidation of the $Sc_xAl_{1-x}N$ films up to 900°C.

Experimental

$Sc_xAl_{1-x}N$ films were grown on epitaxial-grade c-sapphire substrates by co-evaporation of a 99.99% pure Al e-beam source and a 99.9% pure Sc e-beam source in the presence of a 600-W RF nitrogen-plasma generated by an Oxford Applied RF HD25 Atom Source with N_2 gas flows between 0.5 sccm and 2.0 sccm. The deposition was carried out in a well-baked UHV chamber with a base pressure $< 1.3 \times 10^{-10}$ kPa and partial pressure of $H_2O < 1 \times 10^{-12}$ kPa as measured by a residual gas analyzer. Prior to insertion into UHV, the c-sapphire substrates were cleaned with acetone and isopropanol, rinsed in deionized water, and mounted onto a Ta carrier that was heated to 930°C during film deposition using a calibrated BN-graphite radiant heater. A nitrogen plasma exposure process for the bare c-sapphire substrate was used to create an aluminum oxynitride layer which has been shown to induce high-quality epitaxy of (0002) AlN grains on c-sapphire.[30] Briefly, this process consisted of ramping the sample to 930°C in the presence of excited N_2 molecules and N* radicals generated by the plasma source and nitriding the substrate surface for 1 h at 930°C. The RF plasma source was operated with deflection plates to divert N_2^+ ions from impinging at the growth surface. $Sc_xAl_{1-x}N$ films were then immediately deposited onto the oxynitride buffer layer using Sc and Al rates that were monitored by quartz crystal oscillators (QCOs) which were calibrated using x-ray reflectivity and step-surface profilometry film thickness measurements. During and following film growth at 930°C, the film structure was monitored using reflection high energy electron diffraction (RHEED) operating with 35-keV beam energy. The $Sc_xAl_{1-x}N$ films were grown to be either 100-nm-thick or 500-nm-thick, with the latter used for fabrication of SAWR devices by employing a clean-room photolithography process for definition of transducer electrodes and reflectors.[25,26,28,29]

Immediately after deposition, $Sc_xAl_{1-x}N$ films were transferred under UHV to another chamber for x-ray photoelectron spectroscopy (XPS) analysis of film stoichiometry using Al Kα x-ray and a SPECS hemispherical electron analyzer. XPS relative sensitivity factors were determined experimentally using AlN, Al_2O_3, and Sc_2O_3 standards and the film compositions are deemed to be accurate to within −2 at.%. The relative sensitivity factors used for Al, Sc, N, and O were 0.44, 1.19, 1,92, and 1.00, respectively, which includes the transmission function from the SPECS analyzer. Upon removal from vacuum, the films were fully characterized by x-ray diffraction (XRD) using a Malvern Panalytical X'Pert Pro system operating with a hybrid monochromator source for gonio scans, rocking curves, and pole figure measurements. Films were also analyzed by scanning electron microscopy (SEM) using a Zeiss NVision-40 imaging system.

To determine the electromechanical coupling coefficient, k^2, for each $Sc_xAl_{1-x}N$ film, SAWR devices were fabricated using a photolithography lift-off process. The SAWR devices were designed to have an operating frequency of 455 MHz with a wavelength $\lambda = 12$ µm, 125 electrode pairs and 400 reflectors, and the electrodes and reflectors were fabricated using 100-nm $Pt_{0.9}N_{0.1}$ films grown on a 10-nm Zr adhesion layer.[31] To protect the $Sc_xAl_{1-x}N$ film from reacting with the highly basic photoresist developer solution during lift-off, a 10-nm-thick Si_xN_y interfacial layer was deposited onto the $Sc_xAl_{1-x}N$ film surface via standard plasma-enhanced chemical vapor deposition (PE-CVD) prior to SAWR patterning and fabrication. This Si_xN_y layer also served as a high-temperature oxidation barrier as discussed in Oxidation and High-Temperature Stability of $Sc_xAl_{1-x}N$ Films Section. Microwave acoustic responses including the parameter of the SAWR devices were measured using an Agilent vector network analyzer (VNA) and a Cascade RF microprobe station.

Journal : Large 11664 | Article No : 9425 | Pages : 8 | MS Code : 9425 | Dispatch : 11-1-2022

Results and Discussion

Influence of Sc /Al Flux Ratio on $Sc_xAl_{1-x}N$ Film Stoichiometry and Structure

$Sc_xAl_{1-x}N$ films were grown at 930°C on the pre-nitrided c-sapphire substrates using Sc/Al flux ratios ranging from 0.33 to 1.0 at a total metal deposition rate of 0.04–0.06 nm/s. Film growth at 700°C resulted in much poorer epitaxy as determined by XRD rocking curves. Figure 1 shows XRD gonio scans as a function of the Sc/Al flux ratio where the (0002) intensity from the $Sc_xAl_{1-x}N$ grains is normalized to the (0006) c-sapphire substrate intensity for each sample. As the Sc concentration increases, the population of (0002) grains oriented normal to the c-sapphire substrate decreases. The largest decrease in (0002) intensity occurs when the Sc concentration increases from 8 at% to 16 at%, and there is almost no measurable (0002) peak when the Sc concentration reaches 30 at.%. In terms of grain size, the XRD full-width-half-max (FWHM) of the (0002) peak from 100-nm-thick films increases from 0.19° to 0.80° as the Sc concentration increases from 8 at.% up to 30 at.% and the corresponding Scherrer grain size normal to the film neglecting inhomogeneous strain decreases from 35 nm to 10 nm. Figure 1 also shows that the (0002) peak position shifts to higher 2θ values consistent with compressive homogenous strain developing along the (0002) wurtzite axis as the Sc concentration increases.

Accurate measurements of the *c*-axis lattice parameter were obtained from XRD gonio scans, and the *a*-axis lattice parameter was obtained using the (1013) peak position obtained from grazing incidence XRD scans with a 1.5° omega offset. These measured values for the *c*-axis and *a*-axis lattice parameters as well as the *c/a* ratio are shown in Fig. 2 as a function of Sc concentration. Inserting Sc atoms substitutionally into the wurtzite lattice decreases the *c*-axis and increases the *a*-axis, thereby decreasing the *c/a* value compared to 1.59 of the ideal AlN wurtzite lattice. This decrease in *c/a* as Sc is added to the lattice is consistent with other reports[8,19,21,22] although these data are for Sc concentrations above 30 at.%. It has also been reported that a $Sc_xAl_{1-x}N$ rock-salt phase can nucleate when the Sc concentration exceeds –45 at.%.[6–8] At a growth temperature of 930°C, we did not find any evidence by XRD for a rock-salt phase in any of our $Sc_xAl_{1-x}N$ films.

RHEED was used to monitor the crystal structure during film growth to verify that epitaxial growth of (0002)-oriented $Sc_xAl_{1-x}N$ grains was achieved. The RHEED patterns for two $Sc_xAl_{1-x}N$ films grown with Sc/Al flux ratios of 1/3 and 2/3 are shown in Fig. 3. Both patterns show evidence of transmission diffraction through the $(2\bar{1}\bar{1}0)$ crystal planes

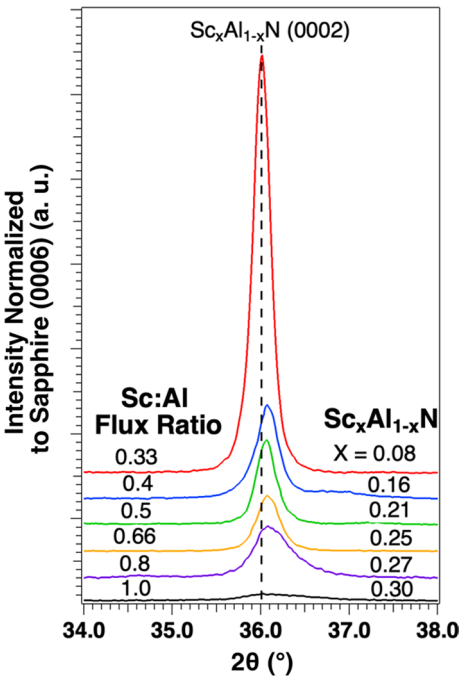

Fig. 1 XRD gonio scans of $Sc_xAl_{1-x}N$ films grown with the Sc/Al flux ratio listed on the left and film stoichiometry as measured by XPS on the right. Increasing the Sc flux relative to the Al flux leads to a reduction in the number of (0002)-oriented grains oriented normal to the film surface.

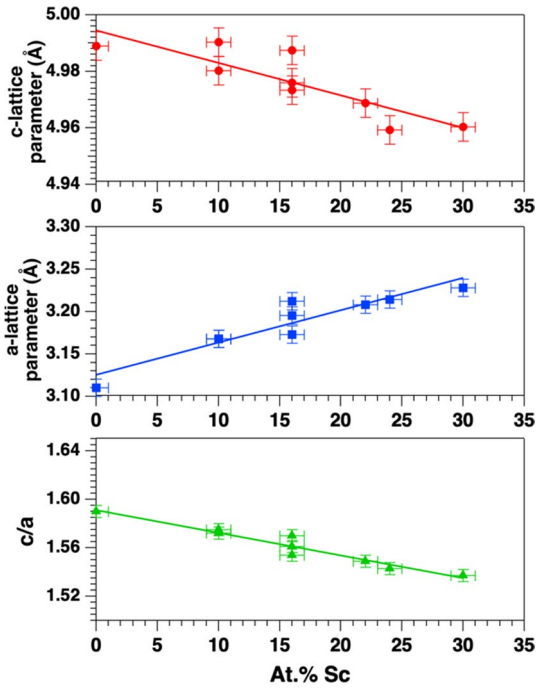

Fig. 2 Lattice constants along the *c*-axis and *a*-axis of the $Sc_xAl_{1-x}N$ wurtzite lattice as measured by XRD as well as the computed *c/a* ratio as a function of Sc content in the film.

Journal : Large 11664 | Article No : 9425 | Pages : 8 | MS Code : 9425 | Dispatch : 11-1-2022

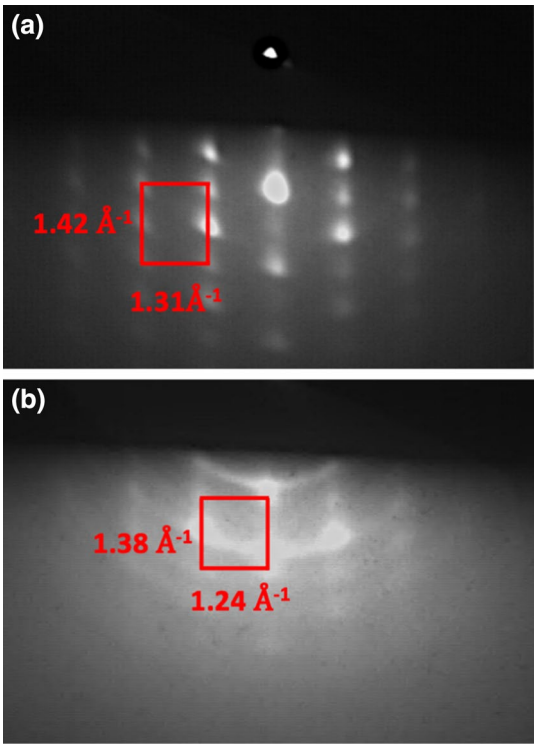

Fig. 3 RHEED patterns acquired during growth of $Sc_xAl_{1-x}N$ films at 930°C. (a) Sc/Al flux ratio = 1/3 that yields a $Sc_{0.10}Al_{0.90}N$ film composition, and (b) Sc/Al flux ratio = 2/3 that yields a $Sc_{0.26}Al_{0.74}N$ composiiton. The RHEED patterns are indexed according to transmission diffraction through (2-1-10) planes of the (0002)-oriented grains. The patterns repeated with every 60° of azimuthal rotation indicating in-plane registry of the grains as well as out-of-plane (0002) epitaxy.

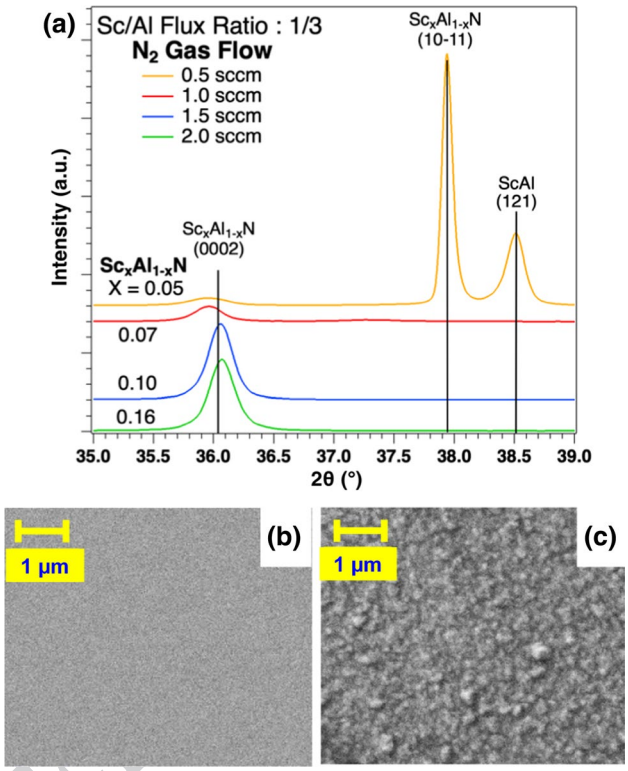

Fig. 4 (a) XRD gonio scans from $Sc_xAl_{1-x}N$ films grown at a Sc/Al flux ratio of 1/3 with a range of N_2 gas flows through the RF plasma source. (b) SEM image from a $Sc_{0.10}Al_{0.90}N$ film grown with a N_2 gas flow of 1.5 sccm. (c) SEM image from a $Sc_{0.07}Al_{0.93}N$ film grown with a N_2 gas flow of 0.5 sccm.

of the highest (0002) oriented $Sc_xAl_{1-x}N$ grains on the film surface, and this transmission diffraction pattern was found to repeat every 60° in concert with the symmetry of the wurtzite lattice indicating in-plane registry of the epitaxial (0002) grains. Figure 3b also shows evidence of rings appearing indicating a loss of (0002) epitaxy as the Sc concentration is increased from 10% to 26%. The horizontal and vertical spacing for the transmission spots were calculated and showed that increase the Sc concentration led to a decrease in horizontal spacing from 1.31Å^{-1} to 1.24Å^{-1} indicating an expansion of the *a*-lattice parameter. The vertical spacing increased from 1.42Å^{-1} to 1.48 Å^{-1} as compression along the *c*-axis occurs.

Effect of Nitrogen Plasma Flux on $Sc_xAl_{1-x}N$ (0002) Film Epitaxy

The nitrogen plasma species generated by an Oxford HD25 RF source operating at 600 W consist of primarily excited N_2 molecules, N* radicals, and N_2^+ ions as determined by optical emission spectroscopy;[32,33] the N_2^+ ions emerging from the source were deflected away from the growth surface in our experiments. By increasing the N_2 gas flow through the RF source, the output flux of the excited N_2 and N* species from the plasma source increases[34] which can impact the reaction rates between Al, Sc, and N adatom species at the growth surface. To investigate the effect of the nitrogen plasma flux, a series of $Sc_xAl_{1-x}N$ films was grown with N_2 gas flows ranging between 0.5 sccm and 2.0 sccm at a Sc/Al flux ratio of 1/3, and they were characterized by XRD gonio scans as shown in Fig. 4. At a low nitrogen plasma flux (i.e. 0.5 sccm), only a minor population of epitaxial $Sc_xAl_{1-x}N$ (0002) grains is produced, and $Sc_xAl_{1-x}N$ (1 0 -1 1) grains and intermetallic ScAl (121) grains also appear. At larger nitrogen plasma fluxes (above 1 sccm) nucleation of non-(0002) grains is inhibited and epitaxial (0002) grains are produced. The surface morphology of $Sc_xAl_{1-x}N$ films grown with gas flows of 1.5 and 0.5 sccm are shown in Fig. 4b and c, respectively, which indicates that film growth under nitrogen-poor conditions leads to the formation of a rougher film as some Sc and Al atoms begin to coalesce into an intermetallic phase.

The stoichiometry of $Sc_xAl_{1-x}N$ films grown under different N_2 gas flows with a constant Sc/Al ratio of 1/3 was

Journal : Large 11664 | Article No : 9425 | Pages : 8 | MS Code : 9425 | Dispatch : 11-1-2022

found to vary. As the N_2 gas flow increased from 0.5 sccm to 2.0 sccm, the Sc concentration in the films increased from 7 at.% Sc to 16 at.% Sc implying that the Sc sticking coefficient depends on the magnitude of the flux from the nitrogen plasma source. Using higher N_2 gas flows leads to more incorporation of Sc atoms into the film and gives another means for controlling the film stoichiometry in addition to adjusting the Sc and Al arrival rates.

Evaluation of Electromechanical Coupling Coefficients of $Sc_xAl_{1-x}N$ Films from SAWR Devices

To evaluate how $Sc_xAl_{1-x}N$ film stoichiometry and nanostructure influences the electromechanical coupling coefficients and hence degree of piezoelectric response, SAWR devices were fabricated from 500-nm-thick $Sc_xAl_{1-x}N$ films grown on c-sapphire substrates using a photolithography lift-off process. The SAW resonators were designed to have an operating frequency near 455 MHz with a wavelength $\lambda = 12\mu m$, an aperture $W = 70$, 125 electrode pairs, and 400 reflectors.[33] SAWR devices were made with $Sc_xAl_{1-x}N$ films having Sc concentrations of 10 at.%, 13 at.%, and 17 at.% as well as pure AlN as a reference. Figure 5a shows the response of the $|S_{11}|$ parameter measured from each of the devices, which shows that the magnitude of the $|S_{11}|$ response increases as the Sc concentration is increased. A small secondary resonant peak located –1.4 MHz below the main resonance is visible for all four films, and this secondary peak is caused by a large device aperture used in the design that allows additional reflection modes to occur. Plotting the conductance (Fig. 5b) and susceptance (Fig. 5c) responses, which eliminates impendence mismatching that can affect $|S_{11}|$ results, also indicate that the acoustic response increases with Sc concentration.

The electromechanical coupling coefficient k^2 for each film was calculated from their conductance and susceptance values[35] which relates to the efficiency of converting between mechanical and electrical energy. Figure 5d shows the XRD intensity of the $Sc_xAl_{1-x}N$ (0002) peak normalized to the sapphire (0006) intensity, and the k^2 values calculated for each of the SAWRs. The degree of (0002) epitaxy decreases with Sc content, consistent with

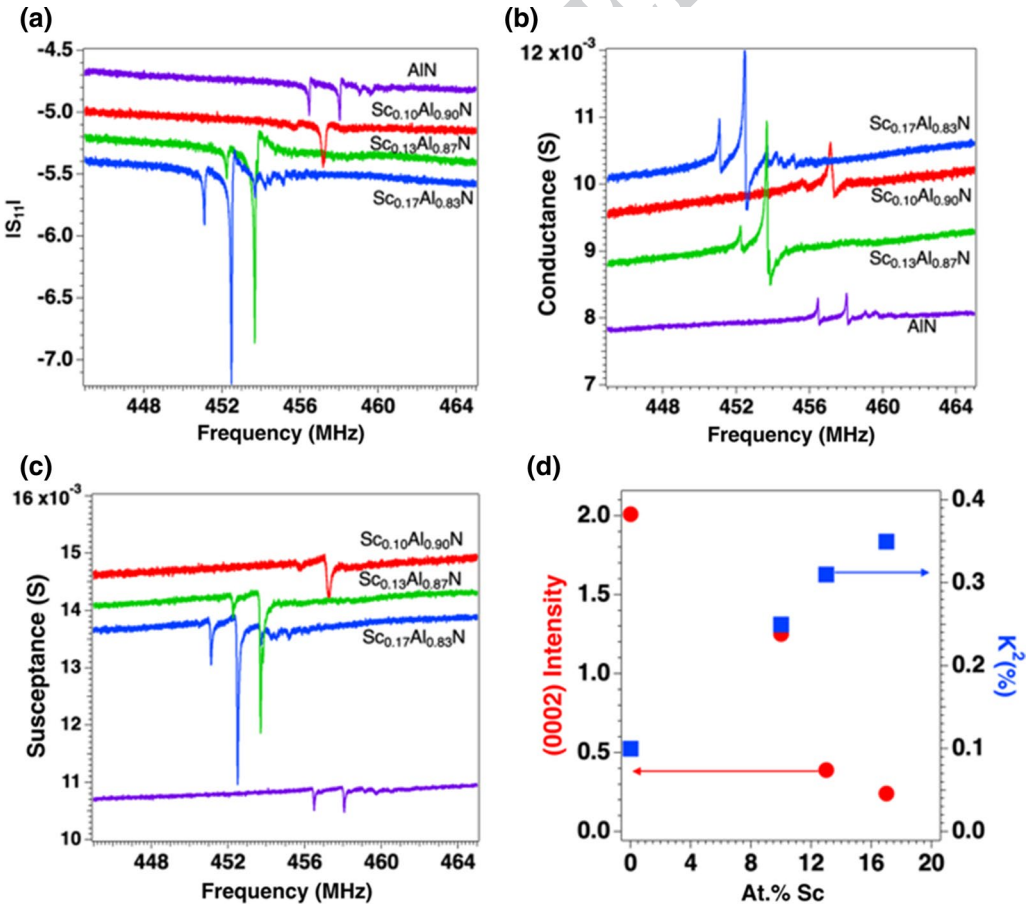

Fig. 5 Microwave acoustic responses from SAWR devices fabricated from different $Sc_xAl_{1-x}N$ film compositions. (a) reflection coefficient $|S_{11}|$, (b) conductivity, (c) susceptance, and (d) XRD (0002) intensity and k^2 plotted versus Sc concentration.

Journal : Large 11664 | Article No : 9425 | Pages : 8 | MS Code : 9425 | Dispatch : 11-1-2022

Fig. 1, but despite this loss in epitaxial quality the value of k^2 is outweighed by the increase in Sc content within the wurtzite lattice. The FWHM of the XRD rocking curves for these samples increased from 1.8° for pure AlN up to 3.27° for $Sc_{0.17}Al_{0.83}N$. This broadening is another indicator of the loss in quality of (0002) epitaxy as the Sc concentration increases. These results suggest that Sc concentration has a stronger influence on piezoelectric coupling than the degree of (0002) epitaxy, although the latter is also an important consideration in obtaining the best piezoelectric performance.

Oxidation and High-Temperature Stability of $Sc_xAl_{1-x}N$ Films

For applications of piezoelectric $Sc_xAl_{1-x}N$-based SAWR devices for wireless sensing in harsh high-temperature environments, the sensor materials need to remain stable under oxidizing conditions up to 1000°C. The high temperature oxidation of AlN films has been extensively studied,[36–42] but little work has been performed concerning high temperature oxidation of $Sc_xAl_{1-x}N$ films. $Sc_xAl_{1-x}N$ is expected to be more prone to oxidation than pure AlN as the formation of Sc_2O_3 has a lower Gibbs free energy of formation than Al_2O_3 over the full temperature range.[27] Thin film capping layers such as Si_xN_y are often used as high-temperature oxidation barriers in microelectronics. For example, Gilinger et al.[42] have showed that a 100-nm-thick Si_xN_y layer is able to severely hinder the oxidation of AlN at 1000°C for 24 h.[42] For our SAWR devices, we have used an ultra-thin 10-nm Si_xN_y layer grown using a standard PE-CVD process to protect the $Sc_xAl_{1-x}N$ film from being etched by the photoresist developer during photolithography. This same 10-nm Si_xN_y capping film also serves as a high-temperature oxidation barrier layer.

Figure 6 shows results from a compound thermal annealing experiment carried out in a box furnace in air up to 900°C. Two 500-nm-thick $Sc_{0.13}Al_{0.87}N$ films, one covered by 10 nm of Si_xN_y and one without, as well as a 500-nm-thick AlN film with the 10-nm Si_xN_y cap, were held at each temperature for 4 h and then cooled to room temperature for XRD analysis. The intensity of the (0002) peak from the XRD gonio scans is shown after each round of heating, and this intensity is normalized to the unheated as-grown (0002) intensity values at 25°C for each sample to show the decrease caused by film oxidation. Up to 800°C, the capped $Sc_xAl_{1-x}N$ and AlN films both show a decrease in (0002) intensity of –15%, whereas the uncapped $Sc_xAl_{1-x}N$ film lost 60% in intensity. Above 800°C, the Si_xN_y capped $Sc_xAl_{1-x}N$ film oxidizes more readily than the Si_xN_y capped AlN film, consistent with the higher thermodynamic driving force for Sc_2O_3 formation compared to Al_2O_3.[27] These results indicate that the thickness of the Si_xN_y capping layer is important for achieving an oxidation barrier that is effective over the long term. The ultra-thin 10-nm Si_xN_y layer has a negligible effect on the performance of the SAWR devices, while using thicker capping layers may impact acoustic propagation and attenuation behavior. Thus, alternative capping layers may also be needed to achieve long-term stability of $Sc_xAl_{1-x}N$ films for high-temperature harsh environment sensing applications.

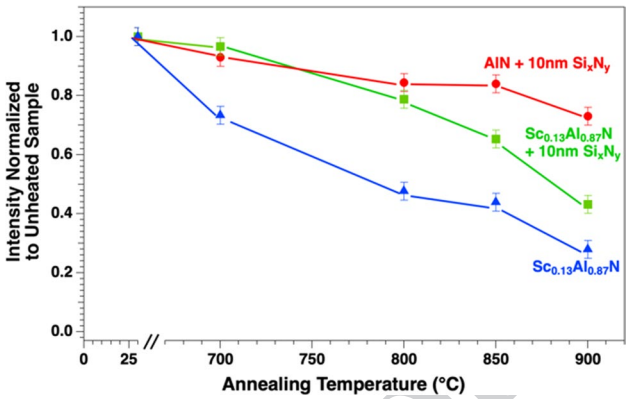

Fig. 6 XRD (0002) gonio scan intensities from a $Sc_{0.13}Al_{0.87}N$ film, a $Sc_{0.13}Al_{0.87}N$ film capped with a 10-nm Si_xN_y layer, and an AlN film capped with a 10-nm Si_xN_y layer following compound annealing in air for 4 h at each temperature. Each of the data points is normalized by the as-grown intensity value at 25°C.

Conclusions

This work has shown that high-quality epitaxial (0002) $Sc_xAl_{1-x}N$ films can be grown on thermally nitrided c-sapphire substrates at 930°C using controlled fluxes of Sc, Al, and N generated by metal evaporation sources and a nitrogen RF plasma source. $Sc_xAl_{1-x}N$ film growth under nitrogen-poor conditions leads to the formation of non-(0002)-oriented $Sc_xAl_{1-x}N$ grains and intermetallic ScAl grains. The best (0002) epitaxy with in-plane registry of the $Sc_xAl_{1-x}N$ grains was achieved using a nitrogen-rich plasma flux and a Sc/Al flux ratio of 1/3 as verified by both XRD and RHEED measurements. Piezoelectric coupling in the $Sc_xAl_{1-x}N$ films was assessed by determining the electromechanical coupling coefficients, k^2, from the measured acoustic response of the SAWR devices at 455 MHz. The magnitude of the k^2 values increase as the Sc concentration increases in the $Sc_xAl_{1-x}N$ films even though increased Sc in the wurtzite lattice leads to poorer film epitaxial (0002) grain alignment. Using a 10-nm Si_xN_y capping layer over the $Sc_xAl_{1-x}N$ films prevents undesired etching by the photoresist developer during SAWR device fabrication and helps hinder oxidation of the $Sc_xAl_{1-x}N$ films up to 800°C.

Journal : Large 11664 | Article No : 9425 | Pages : 8 | MS Code : 9425 | Dispatch : 11-1-2022

Acknowledgments The authors would like to acknowledge the assistance of G. Bernhardt and M. Call from the Frontier Institute for Research in Sensor Technologies (FIRST) at the University of Maine in the fabrication of the SAWR devices. This work was supported by the U.S. Department of Energy - National Energy Technology Laboratory Award #: DE-FE-0031550. *Disclaimer*: This report was prepared as an account of work sponsored by an agency of the United States Government. Neither the United States Government nor any agency thereof, nor any of their employees, makes any warranty, express or implied, or assumes any legal liability or responsibility for the accuracy, completeness, or usefulness of any information, apparatus, product, or process disclosed, or represents that its use would not infringe privately owned rights. Reference herein to any specific commercial product, process, or service by trade name, trademark, manufacturer, or otherwise does not necessarily constitute or imply its endorsement, recommendation, or favoring by the United States Government or any agency thereof. The views and opinions of authors expressed herein do not necessarily state or reflect those of the United States Government or any agency thereof.

Conflict of interest The authors declare that they have no conflict of interest.

References

1. M.B. Assouar, O. Elmazria, M. El Hakiki, and P. Alnot, Study of acoustical and optical properties of AlN films for SAW and BAW devices: correlation between these properties. *Integr. Ferroelectr.* 82, 45 (2006)
2. T. Aubert, O. Elmazria, B. Assouar, L. Bouvot, and M. Oudich, Surface acoustic wave devices based on AlN/sapphire structure for high temperature applications. *Appl. Phys. Lett.* 96, 203503 (2010)
3. T. Palacios, F. Calle, E. Monroy, J. Grajal, M. Eickhoff, O. Ambacher, and C. Prieto, Nanotechnology for SAW devices on AlN epilayers. *Mater. Sci. Eng., B* 93, 154 (2002)
4. L. Shu, J. Jiang, B. Peng, Y. Wang, and X. Liu, AlN film SAW resonator integrated with metal structure. *Electron Lett* 51, 379 (2015)
5. A. Nicoloiu, A. Muller, I. Zdru, D. Vasilache, G.E. Stan, C. Nastase, V. Dumitru, A. Dinescu, AIN/Si based SAW resonators for very high sensitivity temperature sensors. *IEEE Int. Ultra Sym.* (2018), p. 1
6. N. Takeuchi, First-principles calculations of the ground-state properties and stability of ScN. *Phys. Rev. B* 65, 045204 (2002)
7. M. Akiyama, T. Kamohara, K. Kano, A. Teshigahara, Y. Takeuchi, and N. Kawahara, Enhancement of piezoelectric response in scandium aluminum nitride alloy thin films prepared by dual reactive co-sputtering. *Adv. Mater.* 21, 593 (2008)
8. M. Akiyama, K. Kano, and A. Teshigahara, Influence of growth temperature and scandium concentration on piezoelectric response of scandium aluminum nitride alloy thin films. *Appl. Phys. Lett.* 95, 162107 (2009)
9. Z. Hao, M. Park, D. G. Kim, A. Clark, R. Dargis, H. Zhu, A. Ansari, Single crystalline ScAlN surface acoustic wave resonators with large figure of merit ($Q\times k_t^2$). *IEEE MTT-S,* 786 (2019)
10. F. Bartoli, J. Streque, J. Ghanbaja, P. Pigeat, P. Boulet, S. Hage-Ali, N. Naumenko, A. Redjaïmia, T. Aubert, and O. Elmazria, Epitaxial growth of $Sc_{0.09}Al_{0.91}N$ and $Sc_{0.18}Al_{0.82}N$ thin films on sapphire substrates by magnetron sputtering for surface acoustic wave applications. *Sensors* 20, 4630 (2020)
11. W. Wang, P.M. Mayrhofer, X. He, M. Gillinger, Z. Ye, X. Wang, A. Bittner, U. Schmid, and J.K. Luo, High performance AlScN thin film based surface acoustic wave devices with large electromechanical coupling coefficient. *Appl. Phys. Lett.* 105, 133502 (2014)
12. F. Bartoli, M. Moutaouekkil, J. Streque, P. Pigeat, S. Hage-Ali, P. Boulet, H. M'Jahed, O. Elmazria, S. Zhgoon, F. Bartoli, T. Aubert, O. B. Matar, A. Talbi, Theoretical and experimental study of ScAlN/sapphire structure based SAW sensor, *IEEE Sensors*, 1 (2017)
13. S. Fujii, M. Sumisaka, G. Tang, Y. Suzuki, S. Otomo, T. Omori, K.-ya Hashimoto, Highly c-axis-oriented ScAlN thin films deposited using Sc-Al alloy target. *IEEE MTT-S,* 1 (2015)
14. S. Tokuda, S. Takayanagi, M. Matsukawa, T. Yanagitani, Film growth of c-axis tilted ScAlN on the sapphire substrate for SAW devices. *IEEE Int. Ultra Sym.,* 1 (2017)
15. A. Kochhar, Y. Yamamoto, A. Teshigahara, K.-Y. Hashimoto, S. Tanaka, and M. Esashi, Wave propagation direction and c-axis tilt angle influence on the performance of ScAlN/sapphire based SAW devices. *IEEE T. Ultrason. Ferr.* 63, 953 (2016)
16. A. Teshigahara, K. Hashimoto, M. Akiyama, Scandium aluminum nitride: highly piezoelectric thin film for RF SAW devices in multi GHz range. *IEEE Int Ultra Sym,* 1, (2012)
17. V.J. Gokhale, B.P. Downey, M.T. Hardy, E.N. Jin, J.A. Roussos, D.J. Meyer, Epitaxial single-crystal ScAlN on 4H-SiC for high-velocity, low-loss SAW devices. *IEEE 33rd International Conference on Micro Electro Mechanical Systems,* 1262 (2020)
18. A. Nicoloiu, A. Muller, I. Zdru, D. Vasilache, G.E. Stan, C. Nastase, V. Dumitru, A. Dinescu, AlN/Si based SAW Resonators for very high sensitivity temperature sensors. *IEEE Int. Ultra Sym.,* 1 (2018)
19. P. Wang, D.A. Laleyan, A. Pandey, Y. Sun, and Z. Mi, Molecular beam epitaxy and characterization of wurtzite $Sc_xAl_{1-x}N$. *Appl. Phys. Lett.* 116, 151903 (2020)
20. Y. Wang, X. Rong, S. Ivanov, V. Jmerik, Z. Chen, H. Wang, T. Wang, P. Wang, P. Jin, Y. Chen, V. Kozlovsky, D. Sviridov, M. Zverev, E. Zhdanova, N. Gamov, V. Studenov, H. Miyake, H. Li, S. Guo, X. Yang, F. Xu, T. Yu, Z. Qin, W. Ge, B. Shen, and X. Wang, Deep ultraviolet light source from ultrathin GaN/AlN MQW structures with output power over 2 Watts. *Adv. Opt. Mater.* 7, 1801763 (2019)
21. M.T. Hardy, E.N. Jin, N. Nepal, D.S. Katzer, B.P. Downey, V.J. Gokhale, D.F. Storm, and D.J. Meyer, Control of phase purity in high scandium fraction heteroepitaxial ScAlN grown by molecular beam epitaxy. *Appl. Phys. Express* 13, 065509 (2020)
22. M.T. Hardy, B.P. Downey, N. Nepal, D.F. Storm, D.S. Katzer, and D.J. Meyer, Epitaxial ScAlN grown by molecular beam epitaxy on GaN and SiC substrates. *Appl. Phys. Lett.* 110, 162104 (2017)
23. X. Xue, Z. Zhou, B. Peng, M.M. Zhu, Y.J. Zhang, W. Ren, Z.G. Ye, X. Chen, and M. Liu, Review on nanomaterials synthesized by vapor transport method: growth and their related applications. *RSC Adv.* 5, 79249 (2015)
24. R. Boichot, D. Chen, F. Mercier, F. Baillet, G. Giusti, T. Coughlan, M. Chubarov, and M. Pons, Epitaxial growth of AlN on (0001) sapphire: assessment of HVPE process by a design of experiments approach. *Coatings* 7, 136 (2017)
25. S. Leone, J. Ligl, C. Manz, L. Kirste, T. Fuchs, H. Menner, M. Prescher, J. Wiegert, A. Zukauskaite, R. Quay, and O. Ambacher, Metal-organic chemical vapor deposition of aluminum scandium nitride. *Phys. Status Solidi RRL* 14, 1900535 (2020)
26. C. Manz, S. Leone, L. Kirste, J. Ligl, K. Frei, T. Fuchs, M. Prescher, P. Waltereit, M.A. Verheijen, A. Graff, M. Simon-Najasek, F. Altmann, M. Fiederle, and O. Ambacher, Improved AlScN/GaN heterosctructures grown by metal organic chemical vapor deposition. *Semicond. Sci. Technol.* 36, 034003 (2021)
27. J. Casamento, H.G. Xing, and D. Jena, Oxygen incorporation in the molecular beam epitaxy growth of ScxGa1− xN and ScxAl1− xN. *Physica Status Solidi (b)* 257, 190061 (2020)

28. S.C. Moulzolf, R. Behanan, R.J. Lad, M. Pereira da Cunha, Langasite SAW pressure sensor for harsh environments. *IEEE Intl. Ultra Sym*., 1224 (2012)
29. M. Pereira da Cunha, Wireless sensing in hostile environments. *IEEE Intl. Ultra Sym.*, 1337 (2013)
30. M. Pereira da Cunha, T. Moonlight, R.J. Lad, D. Frankel, G. Bernhardt, High temperature sensing technology for applications up to 1000C, *IEEE Sensors*, 752 (2008)
31. G. Bernhardt, C. Silvestre, N. LeCursi, S.C. Moulzolf, D.J. Frankel, and R.J. Lad, Performance of Zr and Ti adhesion layers for bonding of platinum metallization to sapphire substrates. *Sensor Actuators B* 77, 368 (2001)
32. R.E. Feeley, 450°C AlN thin film growth on Nitrided C-plane sapphire substrates. (Ph.D. thesis, University of Maine, 2019)
33. F.U. Khan, N.U. Rehman, S. Naseer, M.A. Naveed, A. Qayyum, N.A.D. Khattak, and M. Zakaullah, Diagnostic of 1356 MHz RF sustained Ar–N2 plasma by optical emission spectroscopy. *Eur. Phys. J-Appl. Phys.* 45, 11002 (2009)
34. Y. Yao, T. Sekiguchi, T. Ohgaki, Y. Adachi, and N. Ohashi, Influence of substrate nitridation on GaN and InN growth by plasma-assisted molecular-beam epitaxy. *J. Ceram. Soc. Jpn.* 120, 513 (2012)
35. W.R. Smith, H.M. Gerard, J.H. Collins, T.M. Reeder, and H.J. Shaw, Analysis of interdigital surface wave transducers by use of an equivalent circuit model. *IEEE T. Microw. Theory* 17, 856 (1969)
36. O. Legrani, T. Aubert, O. Elmazria, A. Bartasyte, P. Nicolay, A. Talbi, P. Boulet, J. Ghanbaja, and D. Mangin, AlN/IDT/AlN/sapphire SAW heterostructure for high-temperature applications. *IEEE T. Ultrason. Ferr.* 63, 898 (2016)
37. R.L. Wang, J.L. Bu, L.X. Yu, Z.F. Wang, and J.L. Sun, Research on oxidation reaction of AlN powder. *Adv. Mat. Res.* 194–196, 1763 (2011)
38. C. Caliendo, and P.M. Latino, Characterization of Pt/AlN/Pt-based structures for high temperature, microwave electroacoustic devices applications. *Thin Solid Films* 519, 6326 (2011)
39. G. Esteves, S.D. Habermehl, P.J. Clews, C. Fritch, and B.A. Griffin, AlN/SiC MEMS for high-temperature applications. *J. Microelectromech. S* 28, 859 (2019)
40. D. Chen, J. Colas, F. Mercier, R. Boichot, L. Charpentier, C. Escape, M. Balat-Pichelin, and M. Pons, High temperature properties of AlN coatings deposited by chemical vapor deposition for solar central receivers. *Surf. Coat. Technol.* 377, 124872 (2019)
41. X. Hou, K.-C. Chou, X. Zhong, and S. Seetharaman, Oxidation kinetics of aluminum nitride at different oxidizing atmosphere. *J. Alloy Compd.* 465, 90 (2008)
42. M. Gillinger, T. Knobloch, A. Marković, G. Pfusterschmied, M. Schneider, and U. Schmid, Performance of thin AlxOy SixNy and AlN passivation layers for high temperature SAW device applications. *Mat. Sci. Semicon. Proc.* 81, 1 (2018)
43. M. Pereira da Cunha, R.J. Lad, T. Moonlight, S.C. Moulzolf, A. Canabal, R. Behanan, P. M. Davulis, D.J. Frankel, G. Bernhardt, T. Pollard, D.F. McCann, *IEEE Sensors*, 41 (2011)
44. S. Yang, Y. Ai, Y. Zhang, Z. Cheng, L. Zhang, L. Jia, B. Dong, B. Zhang, and J. Wang, Impact of device parameters on performance of one-port type SAW resonators on AlN/sapphire. *J Micromech. Microeng.* 28, 085005 (2018)

Journal : **Large 11664** | Article No : **9425** | Pages : **8** | MS Code : **9425** | Dispatch : **11-1-2022**

Journal:	**11664**
Article:	**9425**

Author Query Form

Please ensure you fill out your response to the queries raised below and return this form along with your corrections

Dear Author

During the process of typesetting your article, the following queries have arisen. Please check your typeset proof carefully against the queries listed below and mark the necessary changes either directly on the proof/online grid or in the 'Author's response' area provided below

Query	Details Required	Author's Response
AQ1	Please confirm if the author names are presented accurately and in the correct sequence (given name, middle name/initial, family name). Author 1 Given name: [Mauricio Pereira] Particle name [da] Last name [Cunha]. Also, kindly confirm the details in the metadata are correct.	
AQ2	References [43], [44] are given in list but not cited in text. Please cite in text or delete them from list.	